European Polymer Journal 87 (2017) 231–240

Contents lists available at ScienceDirect

European Polymer Journal

journal homepage: www.elsevier.com/locate/europolj

Effect of the composition and chemical aging in tung oil-styrene networks: Free volume and dynamic-mechanical properties

Carlos Macchi [a,*], Cintia Meiorin [b], Mirna A. Mosiewicki [b], Mirta I. Aranguren [b,*], Alberto Somoza [a]

[a] CIFICEN (UNCPBA-CICPBA-CONICET) and Instituto de Física de Materiales Tandil (UNCPBA), Pinto 399, B7000GHG Tandil, Argentina
[b] Instituto de Investigaciones en Ciencia y Tecnología de Materiales (INTEMA), Universidad Nacional de Mar del Plata (UNMdP) - CONICET, Av. Juan B. Justo 4302, 7600 Mar del Plata, Argentina

ARTICLE INFO

Article history:
Received 28 April 2016
Received in revised form 27 October 2016
Accepted 8 December 2016
Available online 16 December 2016

ABSTRACT

A study on the effect of the composition and chemical aging in tung oil-styrene networks prepared by cationic polymerization is presented. To this aim, the experimental techniques positron annihilation lifetime spectroscopy and dynamic-mechanical analysis were used. The representative experimental parameters were the nanohole free volume, the glass transition temperature and the dynamic mechanical properties, storage and loss moduli and tan δ. The results obtained were discussed in terms of the structure of the formed network, in particular to the packing of the molecular segments and the presence of dangling chains derived from the tung oil. In the case of aged samples the results were interpreted in terms of the oxidative polymerization and degradative processes in the copolymers studied.

1. Introduction

Tung oil-styrene based thermoset polymers (TO-St) have been investigated as an alternative to the production of synthetic networks [1–8]. The resulting bio-based materials have shown to present competitive properties depending on the proportion of the monomers selected, with some formulations displaying shape memory behavior [1,4]. The key parameter determining this last feature is the glass transition temperature of the material (T_g) and its capability of deforming and recovering at higher temperatures.

One additional characteristic of these materials is that they can suffer chemical aging if some double bonds of the tung oil remain unreacted after copolymerization and networking with styrene. The aging process occurs by the action of the oxygen of the surrounding air, which leads to the formation of peroxides, acids, radicals and eventually crosslinking. These changes profoundly affect the glass transition temperature of the materials, as well as their mechanical and dynamic mechanical properties [2]. Thus, a more careful study of this property was pursued.

One key parameter in determining the molecular mobility, and consequently the properties of a polymer, is the free volume. Among many physical techniques available to characterize the open spaces in polymers, Positron Annihilation Lifetime Spectroscopy (PALS) has been able to directly determine the nanohole free volume (radius from about 1 to 10 Å) and its fraction [9].

When an energetic positron emitted from a radioactive source enters into the polymer, it rapidly slows down up to reach the lattice thermal energies; this process is known as thermalization. Then, a positron can annihilate with a free electron or

* Corresponding authors.
E-mail address: marangur@patora.fi.mdp.edu.ar (M.I. Aranguren).

http://dx.doi.org/10.1016/j.eurpolymj.2016.12.016
0014-3057/

form a bound state with an available free electron, known as positronium (Ps). Positronium can be formed in two states according with the different spin orientation of the two particles: antiparallel spins, *para*-positronium (p-Ps) and parallel spins, *ortho*-positronium (o-Ps). In vacuum, p-Ps annihilates into two gamma rays of 511 keV with a lifetime of 125 ps, whereas o-Ps annihilates into three gamma rays with a lifetime of 142 ns. In condensed matter, o-Ps lifetime is influenced by the electron density surrounding it and can be shortened up to few ns (this process is called o-Ps pick-off) and the size of the nano or sub-nanoholes is directly linked to the reduced lifetime of the o-Ps. p-Ps is hardly influenced by the electron of the medium.

The aim of this work is to study the effect of the composition and aging treatments of copolymers prepared by cationic polymerization of tung oil and styrene on the molecular arrangements and dynamic mechanical properties. To achieve this aim positron annihilation lifetime measurements and dynamic-mechanical analysis were performed.

2. Experimental

2.1. Materials

Tung oil, mainly composed of α-eleostearic acid (αEA) triglyceride (84 wt.% of the total fatty acids corresponds to αEA), was supplied by Cooperativa Agrícola Limitada de Picada Libertad, Argentina. Styrene and tetrahydrofurane (THF) were purchased from Cicarelli laboratory, Argentina. Boron trifluoride diethyl etherate ($BF_3.OEt_2$) was obtained from Sigma-Aldrich and used as the initiator of the cationic reaction.

2.2. Cationic copolymerization of TO-St copolymers

A selected amount of St was added to the TO. The mixture was stirred and this step was followed by the addition of the modified initiator prepared by mixing tetrahydrofuran, THF (5 wt.% with respect to the reactive components) with boron trifluoride diethyl etherate (3 wt.% with respect to the reactive components). The mixture was vigorously stirred and finally poured into glass plates of 13 mm × 18 mm. The reactants were heated first at 25 °C for 12 h, then at 60 °C for 12 h and finally at 100 °C for 24 h. TO-St weight ratios of 0/100, 10/90, 30/70, 40/60, 50/50, 60/40, 70/30 and 100/0 were prepared. A scheme of the network structure is shown in Fig. 1.

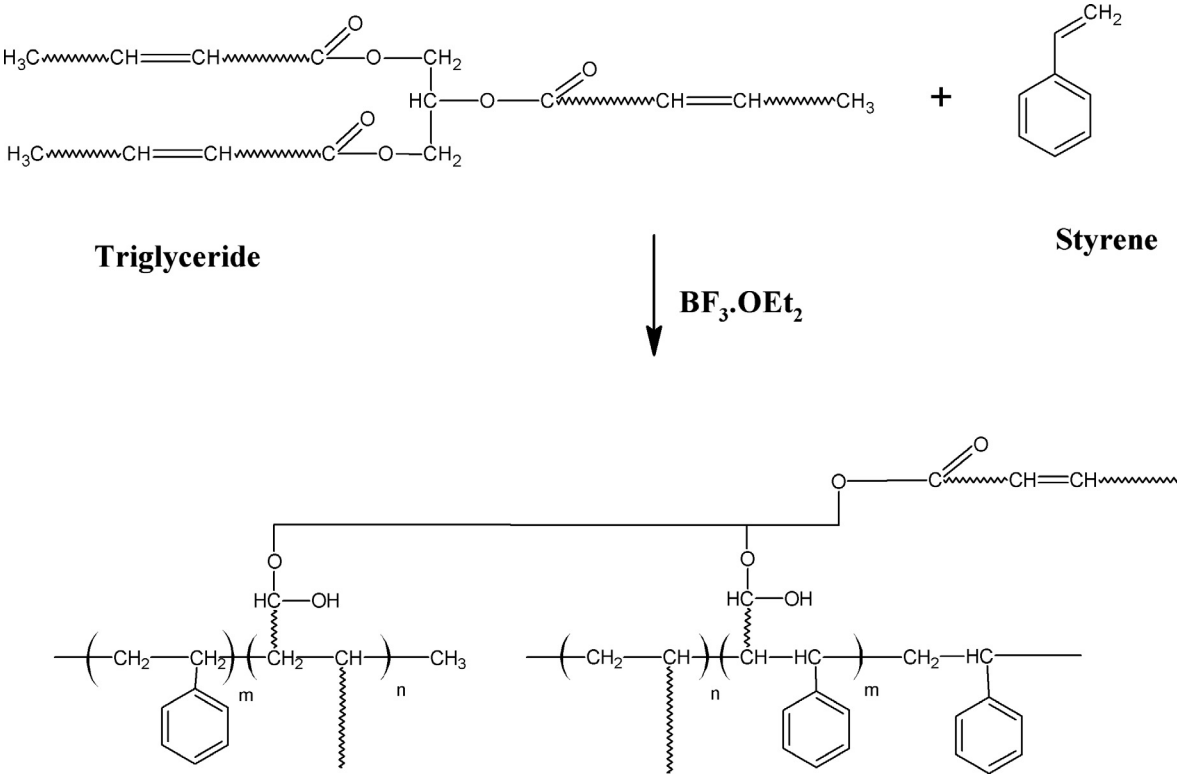

Fig. 1. Scheme of the network structure showing the chemical bonds formed during the co-reaction of tung oil and styrene by cationic polymerization [4].

After reaction, the samples were conditioned at room temperature (RT) in a desiccator containing silica gel to maintain low humidity, in a normally illuminated area. Two kind of samples were mainly studied, those recently prepared (named fresh samples) and those aged for two years at RT (named aged samples).

2.3. Dynamic mechanical tests

A Perkin Elmer dynamic mechanical analyzer (DMA 7) was used to determine the dynamic mechanical behavior of the samples. The tests were carried out under nitrogen atmosphere using the temperature scan mode and a tensile fixture. The chosen dynamic and static stresses were 50 and 100 Pa, respectively. The average sample dimensions were $20 \times 5 \times 0.5$ mm^3. The frequency of the forced oscillations was fixed at 1 Hz and the heating rate was of 10 °C/min. At least two tests for each sample were carried out to check repeatability of the measurements.

The dynamic mechanical properties of the materials were determined from the temperature scans: storage modulus (E′), loss modulus (E″), and tan δ (E″/E′). Because of the simplicity of the method, the T_g of a sample was taken as the temperature at which the maximum in the tan δ peak occurred. It should be remembered that the T_g value is usually several degrees higher than the value determined by other experimental techniques, such as differential scanning calorimetry (DSC). Due to the wide range of temperatures covered by the glass transition of these materials, DSC is not well suited for determining the T_g values of the samples.

2.4. Positron annihilation lifetime spectroscopy (PALS)

2.4.1. PALS system set-up

The positron lifetime spectrometer used consisted on a fast-fast timing coincidence system with a time resolution (FWHM) of 340 ps. At least ten positron lifetime spectra containing 2×10^6 counts each were recorded using a 0.2 MBq sealed source of ^{22}NaCl deposited onto a thin Kapton foil (1.08 mg/cm^2). The source was sandwiched between two identical samples with dimensions $10 \times 10 \times 1.5$ mm^3. The spectra were decomposed into three discrete lifetime components using the LT10 program [10]. Firstly, all samples were measured RT; for those samples which at RT were in the glassy state, additional measurements were performed at a temperature slightly above their corresponding T_g (i.e., in the rubber state).

2.4.2. PALS model

According to the common interpretation of PALS results in polymers, spectra are deconvoluted into three discrete lifetime components. As usual, the shortest lifetime τ_1 (~100 ps) is due to positrons annihilated into the bulk and to p-Ps annihilations while the intermediate component τ_2 (~400 ps) is attributed to "free" positrons annihilated in low electron density regions of the structure. In addition; the longest lifetime component τ_3 (1–5 ns) is ascribed to o-Ps decay in the nanoholes forming the free volume; i.e. $\tau_3 \equiv \tau_{o\text{-}Ps}$.

A correlation between $\tau_{o\text{-}Ps}$ and the size of the hole is possible assuming a spherical approximation of holes of radii R, as expressed using a simple quantum mechanical model; the Tao-Eldrup model [11,12]:

$$\tau_{o-Ps} = 0.5\left[\frac{\Delta R}{R+\Delta R} + \frac{1}{2\pi}\sin\left(\frac{2\pi R}{R+\Delta R}\right)\right]^{-1} \quad (1)$$

where $\tau_{o\text{-}Ps}$ is given in ns and ΔR = 1.66 Å is an empirical parameter valid for materials, such as polymer, containing simple covalent bonds [13]. The average nanohole free volume v_h can then be calculated as

$$v_h = \frac{4}{3}\pi R^3 \quad (2)$$

On the other hand, the total fraction of o-Ps formed $I_3 \equiv I_{o\text{-}Ps}$ is generally related to the number of nanohole free volumes in the material matrix [13].

3. Results and discussion

3.1. Glass transition temperature as a function of the network composition

In a previous work [2], the relationship between T_g (determined from DMA tests) and the composition of the copolymer in fresh and aged samples, was discussed. Fig. 2 shows that T_g increases as the St concentration increases for the recently prepared samples as well as for the aged ones. This trend was related to the decrease of dangling chains ends of high mobility associated with the TO as the St content increases in the copolymer formulation. The reactive unsaturations in the TO are in the carbons 9, 11 and 13 of the eleostearic acid, which is the main fatty acid component of the TO (and consisting of a chain of 18 carbon atoms). When the double bonds react, the tail of the fatty acid chain becomes a dangling chain in the network structure acting as an internal plasticizer of the crosslinked polymer.

Fig. 2 shows that two non aged samples (fresh samples) do not follow the general trend. They correspond to the two formulations with the highest concentrations of TO used in our investigations. It is believed that in these cases the high func-

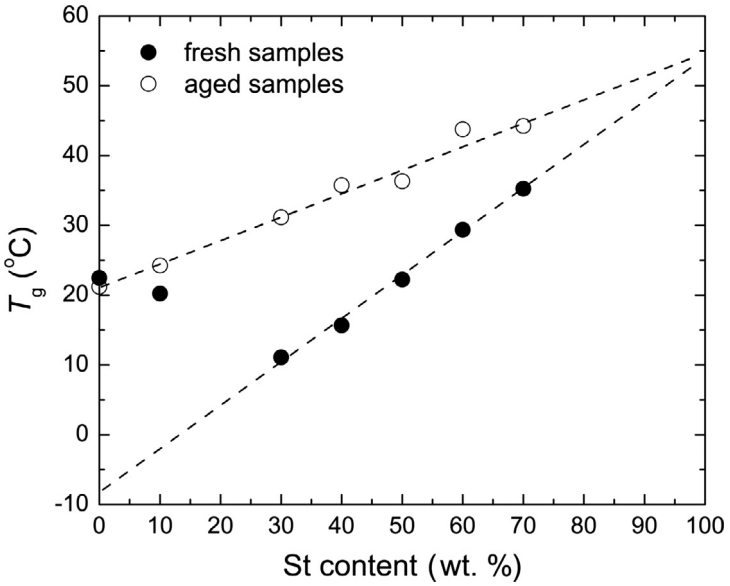

Fig. 2. Glass transition temperature of networks made from the cationic polymerization of tung oil and styrene. Formulations with different concentrations of styrene were considered. Dashed lines are only eye guides.

tionality of the TO contributes to the formation of highly crosslinked networks, a feature that counterbalances the effect of the dangling chains [4]. It must be also added that the obtained networks have very heterogeneous structures mainly in the case of the two samples mentioned, and particularly at 0 wt.% St.

After curing, some carbon-carbon double bonds in the fatty acid chains may remain unreacted, additionally contributing to the presence of dangling chains on the final structure.

Fig. 2 also illustrates that aging occurs strongly affecting the T_g of the samples with a more marked effect as the content of TO increases in the copolymer. This fact indicates that the aging is mainly related to changes in the TO chains that are part of the crosslinked network. Accordingly, it is speculated that some double bonds remained unreacted in the samples during thermal curing and reacted later with the oxygen from the surrounding air. Given enough time, oxygen from the air can diffuse into the sample generating chemical reactions that produce changes in the properties of these materials [14]. Among the most important chemical reactions are those that involve oxidative polymerization and degradative processes [15–18]. These reactions might generate chain scission and formation of volatile products. Additionally, the dangling segments of the fatty acid chains that act as plasticizers in a fresh sample can become part of the network after oxidative chemical reactions, and the mechanical response of the materials can be remarkably enhanced. In the case of the two samples with the lowest amount of St, the heterogeneity of these samples and the rigidity of crosslinking points already formed that could restrict the formation of effective new interchain bonds may be responsible for the negligible changes observed.

3.2. Free volume size dependence on the TO-St network composition

Table 1 summarizes the results of $\tau_{o\text{-}Ps}$ values obtained for the fresh samples measured at RT and for those fresh samples measured in their rubber state at approximately the same temperature above their corresponding T_g. The measurements

Table 1
$\tau_{o\text{-}Ps}$ values for the fresh samples measured at RT and for the same samples measured in their rubber state.

Fresh samples		
Styrene (%)	$\tau_{o\text{-}Ps}$ (ps) @ RT	$\tau_{o\text{-}Ps}$ (ps) @ rubber state
0	2350 ± 15	
10	2320 ± 15	
30	2250 ± 15	
40	2230 ± 10	
50	2147 ± 10	2260 ± 10
60	2085 ± 10	2245 ± 10
70	2077 ± 15	2240 ± 15
100	1990 ± 10	2280 ± 20

were performed at $T_{measurement} = T_g + \Delta T$, where ΔT was about 9 °C and T_g corresponds to the glass transition temperature of the samples. In the case of the recently prepared TO-30wt.%St sample (which has the lowest T_g among all the copolymers studied, see Fig. 2), $T_{measurement}$ corresponds roughly to the RT conditions.

In Fig. 3, the evolution of the calculated v_h with the St content in the different TO-St networks is shown.

In the case of fresh samples measured at RT, v_h shows a linear decrease, within the experimental scatter, when the St content in the copolymer increases. The nanohole free volume varies from ~132 Å^3 for pure TO sample until ~96 Å^3 for pure St. This last v_h value is in good agreement with those reported in the literature for pure polystyrene (PS) [19–21].

In Fig. 3 the v_h values obtained for the copolymers measured in the rubber state are also shown. Arrows indicate the evolution of v_h values when the samples were measured at a temperature ensuring a change in their thermodynamic state; i.e. from the glassy state to the rubber one according to the criterion described in the first paragraph of this section. The same procedure was followed for pure St. It deserves to be mentioned that for samples with a St content higher than 30%, v_h reaches an almost constant value around 123 Å^3. For lower St contents, higher v_h values were obtained.

In Table 2, the obtained $\tau_{o\text{-}Ps}$ values for the aged samples measured at RT and for the aged samples measured in their rubber state are shown. For this kind of samples, measurements in the rubber state were carried out under the same experimental conditions described above for the fresh samples.

In Fig. 4, the evolution of the calculated v_h with the St content for the different TO-St aged networks is shown. In the case of aged samples measured at RT, in the range from the pure TO up to 50 wt.% St, v_h shows a similar behavior, but systematically below than those observed for the fresh samples. Furthermore, an increase of the St content in the formulation of the copolymer, lead to a further decrease of v_h, but this effect occurs at a lower rate. When extrapolating this last stage of the v_h evolution to pure St, a value of the nanohole free volume of about 96 Å^3 is obtained which is in good agreement with that obtained for the pure St sample shown in Fig. 3. This result supports the idea that the changes related to aging occur in the tung oil segments.

Following the same procedure previously described for fresh samples, aged samples were measured in the rubber state. As already mentioned in the description of Fig. 3, arrows indicate the increase of v_h when the thermodynamic state of the sample is changed. The final v_h values reported in the figure are almost identical to those presented in Fig. 3. The interpretation of this result is discussed below.

Studying triglycerides using positron techniques, Nishchenko et al. [22] found a bimodal distribution of the nanohole size in these materials. While the larger holes were related to "cages" near the polar glycerol part of the molecular structure that links the three fatty acids, the smaller ones appear to be related to "cages" formed between the non-polar chain ends. In our case, the obtained v_h values are closer to the values reported by these authors for the smaller nanoholes. This would suggest that in the TO-St copolymers studied in this work the average nanohole size is mainly related to the regions of the non-polar hydrocarbon chains that constitute the dangling chains of these materials (approximately from C13 –C18 for the crosslinked chains). As the amount of styrene is increased in the formulation, the oil insaturations are linked via St chains. As St-St chains become more and longer, they form well packed segments that reduce the nanohole size at RT and the mobility of the

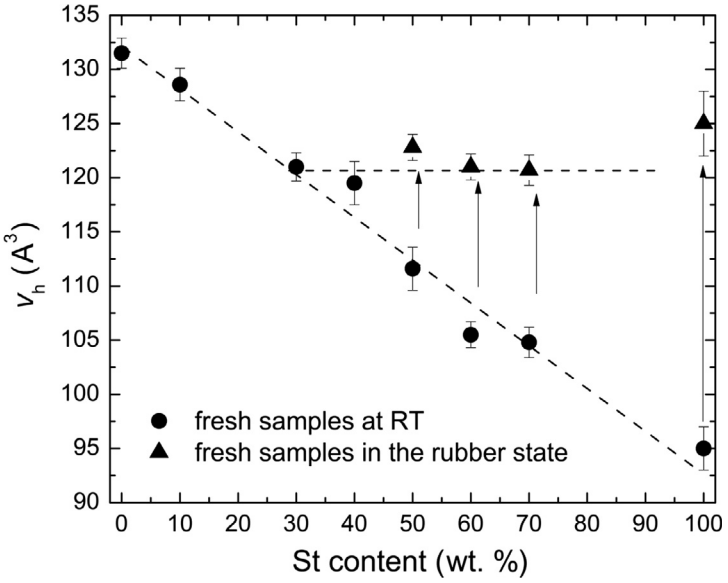

Fig. 3. Size of the free volume holes as a function of the composition of the copolymer. (●) Fresh samples measured at room temperature; and (▲) Fresh samples measured above their corresponding T_g. Dashed lines are only eye guides. Arrows indicate the change of v_h when the samples were measured in the rubber state (see text).

Table 2
$\tau_{o\text{-}Ps}$ values for the aged samples measured at RT and for the aged samples measured in their rubber state. In the last column, $\tau_{o\text{-}Ps}$ values for the thermally refreshed ("rejuvenated") samples measured at RT are also shown.

Styrene (%)	Aged samples		Refreshed samples
	$\tau_{o\text{-}Ps}$ (ps) @ RT	$\tau_{o\text{-}Ps}$ (ps) @ rubber state	$\tau_{o\text{-}Ps}$ (ps) @ RT
0	2230 ± 25		
10	2200 ± 20	2275 ± 15	
30	2107 ± 15	2255 ± 15	2117 ± 15
40	2075 ± 30	2265 ± 10	2065 ± 15
50	2040 ± 20	2245 ± 15	1995 ± 15
60	2035 ± 15	2220 ± 20	2035 ± 15
70	2030 ± 15	2270 ± 15	

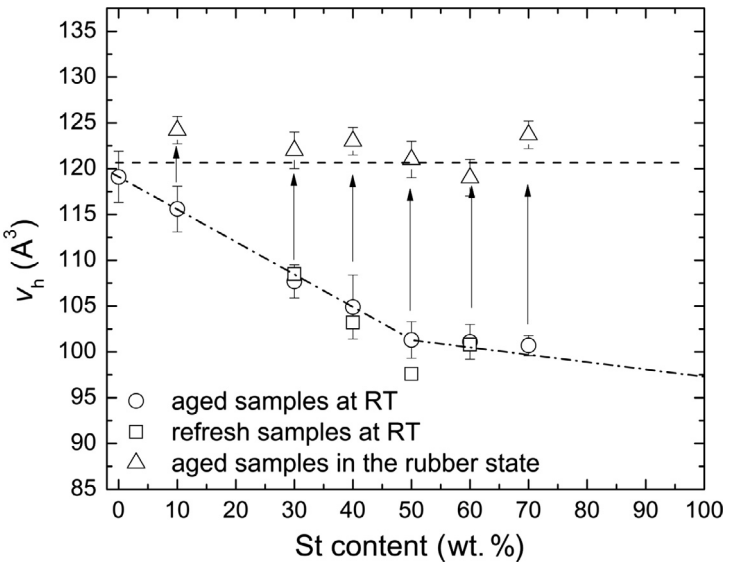

Fig. 4. Size of the free volume holes as a function of the composition of the copolymer. (○) Aged samples measured at room temperature; (△) Aged samples measured above their corresponding T_g; and (□) Refreshed samples at room temperature (see text). Dashed lines are only eye guides. Arrows indicate the change of v_h when the samples were measured in the rubber state (see text).

polymer (above 30 wt.% St). However, if heated at a temperature close but above the T_g of the sample, the St segments recover mobility and the "cages" involving the chain ends, recover the original size, that of the chain ends regions at the rubber state. This would explain why all the samples show the same nanohole free volume value, within the experimental scatter, at a temperature slightly above the T_g of each sample. It also explains why the size of the nanohole is also equal for the fresh or aged samples, independently of further crosslinking due to the oxydation process.

The larger volume measured for the fresh samples with no St or just 10 wt.% St, is probably the result of the heterogeneous structure of these networks and probably to a metastable free volume in the triglyceride (not uncommon in these materials) that is fixed through the crosslinking. The oxidation process during aging and stabilization of the sample takes the nanohole size assigned to the movement of the chain ends as explained before. The effect of the aging process was further investigated.

A priori, aging could be due to physical densification of the material or to chemical changes produced during storage. To distinguish between the two possible effects, some aged samples were re-heated above their T_g (temperature selected = 70 °C) for half an hour and then cooled down to RT under vacuum. Finally, these refreshed samples (or rejuvenated samples) were characterized again by PALS and those results are also presented in Fig. 4. From the analysis of the results reported in the figure, it can be concluded that the refreshing treatment did not appreciably influence the v_h values. This observation strongly supports the conclusions of a previous publication [2] based on the T_g results (and FTIR spectra of the samples) regarding the chemical nature of the aging process experienced by these materials. Unsaturated fatty acids (and vegetable oils) can undergo reactions with atmospheric oxygen, which lead to oxidation, chain scission and polymerization. This feature is typical of drying oils, such as the tung oil used in this study. If polymerization (or chain scission of dangling chains leading to rearrangement of the network structure) is prevalent, it is expected that when the v_h of the material is reduced T_g increases.

Comparison of Figs. 2–4 clearly illustrates that as the wt.% of St increases, the size of the nanohole is reduced (less dangling chains, and a better packed structure of the materials richer in St). This trend, added to the increased rigidity of the aromatic styrene segments, compared to the aliphatic chains in the vegetable oil, are responsible for the increased T_g of the materials.

The lower values of v_h measured for the aged samples with respect to the fresh ones also agree with the higher T_g values measured in the aged materials.

PALS results show that aging produces a reduction of the nanohole size forming the free volume; however, for the samples without St and with 10 wt.% St a simple correlation with T_g cannot be observed, which is probably due to the already mentioned heterogeneity of these networks.

3.3. Ps formation

In Fig. 5, the evolution of the o-Ps intensity as a function of the St content (lower axis) and TO content (upper axis) in the copolymer is presented. As can be seen in the figure, for all the states of the samples $I_{o\text{-}Ps}$ systematically increases as the St content increases (or TO content decreases). The $I_{o\text{-}Ps}$ values for the fresh samples are systematically above to those corresponding to the aged and the refreshed samples. Significant differences in the intensity values for the aged and refreshed samples respectively are not observed. It must be pointed out that, within the experimental scatter, the $I_{o\text{-}Ps}$ values does not vary when the thermodynamic state of the samples is changed.

A similar evolution of $I_{o\text{-}Ps}$ as a function of the composition of analogous systems made from styrene polymer and modified by the addition of other comonomers, such as styrene-maleic anhydride copolymer and styrene-acrylonitrile copolymer, chromosphore in polymethylmethacrylate (PMMA), polyisoprene-tetramethylthiuram disulfide was reported in Refs. [19,23,24]. This behavior was attributed to the presence of chemical species (maleic anhydride, acrylonitrile, chromosphore and tetramethylthiuram disulfide) in the systems that partially inhibit the Ps formation by scavenging electrons. It was also found that the inhibition effect is dependent on the concentration of the inhibiting species. Besides, under this effect $I_{o\text{-}Ps}$ cannot longer be related to the number of nanohole free volumes in the material matrix [25]. On the other hand, inhibition of Ps formation competes with a number of other processes such as spin conversion [26].

Following ideas reported in the literature [19], the decrease of $I_{o\text{-}Ps}$ with the increase of the St concentration (see Fig. 5) was mainly attributed to the presence of inhibiting species that, in our case, were assumed to be related to TO such as radicals and carbonyl groups that act as electron scavengers [2,27,17,28–31]. Furthermore, in Fig. 5 it can be seen that the intensity data corresponding to aged samples are systematically below than those of the fresh samples allowing us to conclude that aging treatment increases the efficiency of the inhibition in the Ps formation. This behavior can be assigned to the production of new chemical species that, as mentioned above, act as electron scavengers.

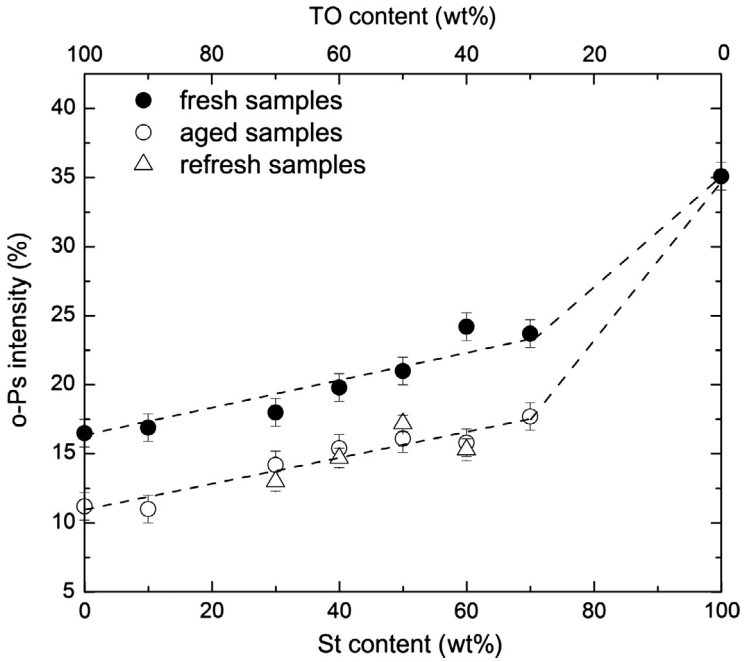

Fig. 5. Intensity of the lifetime associated with the o-Ps lifetime component as a function of the concentration of styrene in the copolymer formulation. Dashed lines are only guide-eyes.

3.4. Temperature and composition effects on the storage modulus of the networks

Fig. 6 shows the important effect of the mobility of the chains, related to the size of the nanohole on the storage modulus (E') of the materials.

At temperatures below the corresponding T_g of each sample, E' depends mostly on the density of the material, which is related to the crosslinking density (not always in a direct way) and the efficiency of the packing of the chains [32]. In this temperature range, the mobility is very low and the glassy modulus is high. The figure illustrates that this dynamic mechanical property is not sensitive to the changes in the formulation or to the effect of oxidation in the materials.

On the other hand, at temperatures above the glass transition, E' is mainly a function of the crosslinking density and of the rigidity of the chains involved in the structure of the networks. From the plotted results, it is clear that for these materials the storage modulus is mainly dependent on the crosslinking density. As the concentration of St (bifunctional monomer) is increased in the formulation, the storage modulus is reduced; i.e., a negative exponential functionality of the E'_{rubber} with the wt.% St is displayed. The same trend is observed in fresh and aged samples, despite the fact that there is not an important difference between each other's values, this behavior indicates that although aging affects T_g, it has a negligible effect on the rubber modulus.

It was already discussed that the oxidation of the materials led to the reduction of υ_h, but it appears that the concentration of elastically active chains (mostly comprised of St-St sequences at moderated and high St concentration, as well as short segments of fatty acid chains between ester groups and reacted double bonds) are not much affected by aging.

Finally, in Fig. 6 are also shown the values measured for the storage modulus of the samples at RT (T = 22 °C), the temperature at which PALS measurements were carried out. In Fig. 7, the results of the fresh samples are replotted as a function of the size of the nanoholes and they show the same overall trend that the one observed for the E′ variation with the St content. These results stress the importance of T_g (or chain mobility and υ_h) on the RT properties of these materials. The presence of TO in the networks plays two opposite effects, that of the dangling chains (which contribute to the increase of υ_h) and that of crosslinking density (which theoretically has the opposite effect). At low wt.% St the storage modulus at RT drops with increasing the St concentration in the formulation of the copolymer, because of the reduction of the crosslinking density, but the modulus increases again when more St is added to the formulation. This effect can be attributed to the reduction of the dangling chains and the improved packing of the chains. This last effect can also be attributed to the reduction of υ_h with increasing wt.% St in the formulations (also related to the better packing of the chains). It should also be considered that the aromatic St molecules incorporated in the network are more rigid than the aliphatic segments provided by the tung oil. St-St segments may require nanoholes of larger sizes to relax; thus the increase of the St content reduces mobility because of the improved packing and high rigidity of the segments which lead to increased modulus. Because of the opposite effects, there is a minimum in the curve of the E' versus υ_h at RT, which corresponds to the two samples with lower T_g. Understanding this effect is of importance for the use of these materials at RT, and help to explain the variation of the mechanical properties most frequently measured at that condition.

As for the aged samples, it was already shown that T_g of the sample with no St (0 wt.% St) was atypical in some aspects and no big change was observed during aging. Consequently, the RT storage modulus did not appreciably change with aging, and essentially the same value was measured for the fresh and aged samples (see Fig. 7).

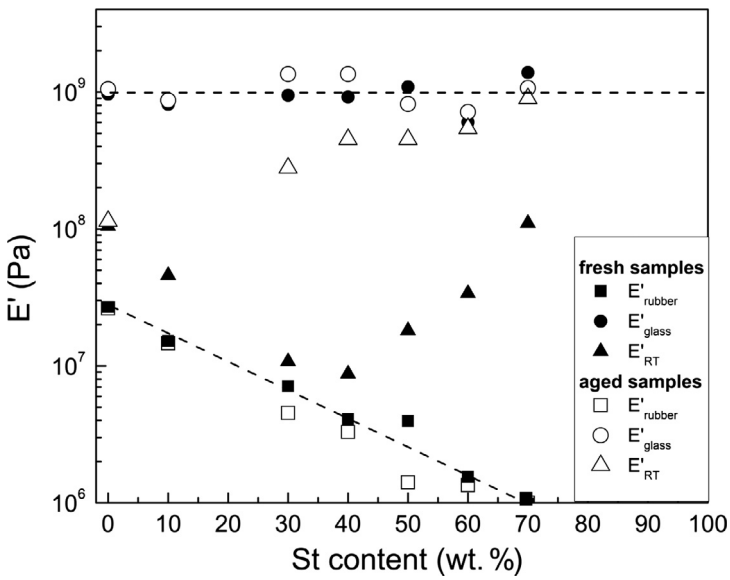

Fig. 6. Storage modulus of the materials in the glassy region, rubbery region and at room temperature. Lines are only eye guides.

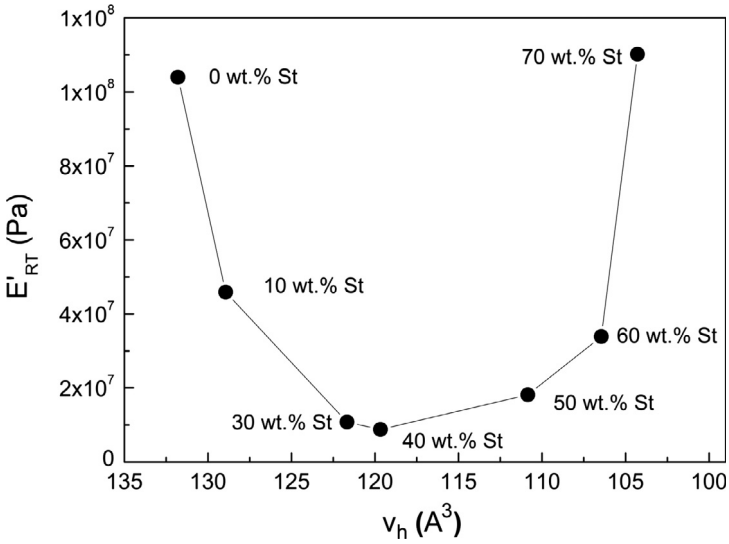

Fig. 7. Storage modulus at RT as a function of the size of the nanoholes.

4. Conclusions

From the results reported in the present work, it can be concluded that:

- The increase of the styrene concentration in the copolymer produces a decrease of the nanohole free volumes as a consequence of a diminution of the dangling chains and a better packed structure of the networks richer in St. This trend, together with the rigidity of the aromatic St segments compared to the aliphatic chains in the tung oil, is reflected in the corresponding increase of the glass transition temperature.
- During aging, for all samples it was observed that v_h decreases while T_g increases. This behavior is attributed to chemical changes linked to oxidative polymerization and degradative processes in the network structure mainly related to TO.
- Independently of their aging condition (fresh or aged), for samples of the copolymers containing more than 30 wt.% St measured in the rubbery state at a temperature slightly above T_g; within the experimental scatter, the same nanohole free volume value was obtained. This result could be explained considering that at a temperature close but above Tg, St segments recover their mobility and nanoholes recover their original sizes, that of the chain end regions at the rubber state
- Glassy and rubber storage modulus are not significantly affected by aging in the materials. However, the trend of the storage modulus measured at RT is in agreement with the observed trend in the nanohole free volumes denoting the effect of T_g on the evaluated properties.
- Additionally, from PALS results it can be concluded that: i) Tung oil partially inhibits the Ps formation; this phenomenon was assigned to the presence of radicals and carbonyl groups in the TO-St copolymer. ii) The aging process occurring through sample-oxygen reactions enhances the efficiency of the Ps inhibition effect, which arises from the production of new chemical species as those mentioned in the previous item.

Acknowledgments

We acknowledge funding from the Agencia Nacional de Promoción Científica y Tecnológica (Argentina) (PICT 2011-1088), Consejo Nacional de Investigaciones Científicas y Técnicas (Argentina) (PIP #114-201101-00151), Comisión de Investigaciones Científicas de la Provincia de Buenos Aires, SECAT (UNCPBA) and Universidad Nacional de Mar del Plata. The authors also thank the Cooperativa Agrícola de Picada Libertad for supplying the tung oil.

References

[1] C. Meiorin, M.I. Aranguren, M.A. Mosiewicki, Smart and structural thermosets from the cationic copolymerization of a vegetable oil, J. Appl. Polym. Sci. 124 (6) (2012) 5071–5078.
[2] C. Meiorin, M.A. Mosiewicki, M.I. Aranguren, Ageing of thermosets based on tung oil/styrene/divinylbenzene, Polym. Test. 32 (2) (2013) 249–255.
[3] C. Meiorin, M.I. Aranguren, M.A. Mosiewicki, Polymeric networks based on tung oil: Reaction and modification with green oil monomers, Eur. Polym. J. 67 (2015) 551–560.

[4] C. Meiorin, M.I. Aranguren, M.A. Mosiewicki, Vegetable oil based thermoset copolymers with shape memory behavior and damping capacity, Polym. Int. 61 (5) (2012) 735–742.
[5] C. Meiorin, D. Muraca, K.R. Pirota, M.I. Aranguren, M.A. Mosiewicki, Nanocomposites with superparamagnetic behavior based on a vegetable oil and magnetite nanoparticles, Eur. Polym. J. 53 (1) (2014) 90–99.
[6] F. Li, R.C. Larock, Synthesis, structure and properties of new tung oil - Styrene - Divinylbenzene copolymers prepared by thermal polymerization, Biomacromolecules 4 (4) (2003) 1018–1025.
[7] F. Li, R.C. Larock, Thermosetting polymers from cationic copolymerization of tung oil: synthesis and characterization, J. Appl. Polym. Sci. 78 (2000) 1044–1056.
[8] S. Bhuyan, S. Sundararajan, D. Andjelkovic, R. Larock, Effect of crosslinking on tribological behavior of tung oil-based polymers, Tribol. Int. 43 (4) (2010) 831–837.
[9] S.J. Tao, Positronium annihilation in molecular substances, J. Chem. Phys. 56 (1972) 5499–5510.
[10] J. Kansy, Microcomputer program for analysis of positron annihilation lifetime spectra, Nucl. Instrum. Meth. A 374 (1996) 235–244.
[11] M. Eldrup, D. Lightbody, N.J. Sherwood, The temperature dependence of positron lifetimes in solid pivalic acid, Chem. Phys. 63 (1981) 51–58.
[12] H. Nakanishi, S.J. Wang, Y.C. Jean, Microscopic surface tension studied by positron annihilation, in: S.C. Sharma (Ed.), Proceedings of International Conference on Positron Annihilation in Fluids, World Scientific, Singapore, 1988, pp. 292–298.
[13] P.E. Mallon, Application to polymers, in: Y.C. Jean, P.E. Mallon, D.M. Schrader (Eds.), Principles and Applications of Positron & Positronium Chemistry, World Scientific, Singapore, 2003, pp. 253–280.
[14] N.J. Fox, G.W. Stachowiak, Vegetable oil-based lubricants – a review of oxidation, Tribol. Int. 40 (7) (2007) 1035–1046.
[15] J. Mallégol, J. Lemaire, J.L. Gardette, Drier influence on the curing of linseed oil, Prog. Org. Coat. 39 (2–4) (2000) 107–113.
[16] M. Lazzari, O. Chiantore, Drying and oxidative degradation of linseed oil, Polym. Degrad. Stabil. 65 (2) (1999) 303–313.
[17] E. Ioakimoglou, S. Boyatzis, P. Argitis, A. Fostiridou, K. Papapanagiotou, N. Yannovits, Thin-film study on the oxidation of linseed oil in the presence of selected copper pigments, Chem. Mater. 11 (8) (1999) 2013–2022.
[18] M.A. Mosiewicki, O. Rojas, M.R. Sibaja, J. Borrajo, M.I. Aranguren, Aging study of linseed oil resin/styrene thermosets and their composites with wood flour, Polym. Int. 56 (7) (2007) 875–881.
[19] C. Wästlund, F.H.J. Maurer, Free-volume properties of styrene-maleic anhydride and styrene-acrylonitrile copolymers, Polymer 39 (1998) 2897–2902.
[20] H.-L. Li, Y. Ujihira, A. Nanasawa, Estimation of free volumes of Polystyrene by positron annihilation lifetime technique, Kobunhi Ronbunshu 53 (1996) 358–365.
[21] K. Ito, Y. Ujihira, Positronium diffusion in polystyrene at low temperatures, Polym. J. 30 (1998) 566–570.
[22] M.M. Nishchenko, S.P. Likhtorovich, D.V. Schur, A.G. Dubovoy, T.A. Rashevskaya, Positron annihilation in C-fullerites and fullerene-like nanovoids, Carbon 41 (2003) 1381–1385.
[23] P.E. Mallon, C.M. Hang, H. Chen, R. Zhang, M.H.S. Gradwell, Y.C. Jean, Positron Annihilation Lifetime Spectroscopy (PAL) as a Tool to Study Rubber (Polyisoprene) Vulcanizate Network Structures, Mat. Sci. Forum 281 (2001) 363–365.
[24] C.M. Huang, E.W. Hellmuth, Y.C. Jean, Positron Annihilation Studies of Chromophore-Doped Polymers, J. Phys. Chem. B 102 (14) (1998) 2474–2482.
[25] M. Eldrup, V.P. Shantarovich, O.E. Mogensen, Inhibition of Ps formation by strong Ps quenchers, Chem. Phys. 11 (1975) 129–142.
[26] O.E. Mogensen, Spur reaction model of positronium formation, J. Chem. Phys. 60 (1974) 998–1004.
[27] U. Ravasio, G. Consolati, A. Faucitano, M. Mariani, F. Quasso, Effects of oxygen in gamma irradiated aromatic polyesters in film, Eur. Polym. J. 43 (2007) 2550–2556.
[28] A. Schönemann, H.G.M. Edwards, Raman and FTIR microspectroscopic study of the alteration of Chinese tung oil and related drying oils during ageing, Anal. Bioanal. Chem. 400 (4) (2011) 1173–1180.
[29] http://wwwpub.iaea.org/MTCD/publications/PDF/te_1617_web.pdf.
[30] A. Buttafava, G. Consolati, M. Mariani, F. Quasso, U. Ravasio, Effects induced by gamma irradiation of different polyesters studied by viscometry, thermal analysis and positron annihilation spectroscopy, Polym. Degrad. Stab. 89 (2005) 133–139.
[31] N. Qi, Z.Q. Chen, A. Uedono, Molecular motion and relaxation below glass transition temperature in poly(methylmethacrylate) studied by positron annihilation, Radiat. Phys. Chem. 108 (2015) 81–86.
[32] L. Rey, J. Galy, H. Sautereau, G.P. Simon, W.D. Cook, PALS free volume and mechanical properties in dimethacrylate-based thermosets, Polym. Int. 53 (2004) 557–568.